Quantification of cyclic and linear flows in plants

Pierre Joliot* and Anne Joliot

Institut de Biologie PhysicoChimique, Centre National de la Recherche Scientifique, Unité Propre de Recherche 1261, 13 Rue Pierre et Marie Curie, 75005 Paris, France

Contributed by Pierre Joliot, February 14, 2005

A method was developed to quantify the fraction of photosystem I (PSI) centers that operate according to the cyclic or linear mode, respectively. P_{700} and plastocyanin oxidation were analyzed under a weak far-red excitation (approximately eight photons per s^{-1} per PSI) that induces P_{700} oxidation in ≈20 s and ≈3 s in dark-adapted and preilluminated leaves, respectively. This finding implies that, in dark-adapted leaves, most of the electrons formed on the stromal side of PSI are transferred back to PSI through an efficient cyclic chain, whereas in preilluminated leaves, electrons are transferred to NADP and then to the Benson–Calvin cycle. Preillumination thus induces a transition from the cyclic to the linear mode. A reverse transition occurs in the dark in a time that increases with the duration and intensity of preillumination. After a ≈10-min illumination under strong light that activates the Benson–Calvin cycle, the transition from the linear to the cyclic mode is completed in >1 h ($t_{1/2}$ ≈ 30 min). The fraction of PSI involved in the cyclic process in dark-adapted leaves can be close to 100%. An apparent equilibrium constant of ≈4 between P_{700} and plastocyanin was measured during the course of the far-red illumination. This value is much lower than that computed from the midpoint redox potential of the two carriers (≈30). These results are interpreted assuming that chloroplasts include isolated compartments defined on the basis of the structural organization of the photosynthetic chain proposed by Albertsson [Albertsson, P. A. (2001) *Trends Plant Sci.* 6, 349–354].

cyclic process | leaf | photosynthetic chain | photosystem I

Occurrence of a cyclic electron flow was first established by Arnon *et al.* (1) who demonstrated that illumination of thylacoids under anaerobic conditions induces ATP synthesis in the presence of vitamin K through a process exclusively recruiting photosystem I (PSI) and cytochrome b_6/f (cyt bf) complexes. Later, Tagawa *et al.* (2) demonstrated that ferredoxin (Fd), a physiological soluble PSI acceptor, was able to catalyze an efficient cyclic phosphorylation, suggesting that a similar process occurs *in vivo*.

A rate for the cyclic process of few s^{-1} has been determined by measurements of P_{700}^+ reduction rate after a far-red illumination (3, 4) or by photoacoustic techniques (4). The presence of a transient rise (tens of seconds time range) in fluorescence after illumination (5, 6) has been attributed to the reduction of the plastoquinone (PQ) pool by electrons originating from the stroma, likely by means of NADPH dehydrogenase (NDH). We have measured (7, 8) the rate of the cyclic flow in leaves submitted to a saturating illumination by measuring the rate of membrane potential decay at the time the light is switched off. In the case of dark-adapted leaves, a rate as high as ≈130 s^{-1} remains for >10 s of illumination. NADPH dehydrogenase that is present at a concentration of few percentages of PSI in thylacoids membranes (9) cannot be involved in such a fast process that operates at a rate close to the rate of linear flow. A likely hypothesis is that electrons are transferred from PSI to the stromal side of cyt bf complex by a process catalyzed by Fd similar to that characterized by Tagawa *et al.* (2). We have proposed (8) a mechanism in which electrons are transferred from the stromal side of cyt bf to the Q_i site, via an electron pathway that involves the high-spin cyt c'_i recently identified in the vicinity of cyt b_h (10, 11). In the presence of 3-(3,4-dichlorophenyl)-1,1-dimethylurea, the cyclic process transiently operates at rate similar to that observed in the absence of PSII inhibitors. The rate falls to value close to zero after a few seconds of saturating illumination, owing to slow electron leaks toward the Benson–Calvin cycle (7, 8) or to oxygen (Mehler reaction). Interestingly, it has been shown that Fd-NADP oxidoreductase (FNR) is able to form a complex with cyt bf (12, 13), which could provide a binding site for Fd on the stromal side of cyt bf. Based on the finding of a small hydrophilic protein (PSI-E) involved in the binding of FNR to PSI (14–16) that increases the efficiency of $NADP^+$ reduction (17), we proposed (8) that PSI–FNR complexes transfer electrons to the Benson–Calvin cycle, and thus, are specifically involved in the linear pathway (PSI_{linear}). On the contrary, PSI not associated with FNR are only able to transfer electrons to the soluble pool of Fd and are specifically involved in the cyclic process (PSI_{cyclic}).

Analysis of the redox state of the photosynthetic electron carriers in chloroplasts submitted to a subsaturating illumination shows that these carriers are not in thermodynamic equilibrium. An equilibrium constant much lower than that derived from the redox potential of the carriers has been measured between Q_A and P_{700} (18), plastocyanin (PC), cyt f and P_{700} (19, 20), or Q_A and PQ (21–23). As discussed in ref. 24, apparent low equilibrium constants are observed between carriers included in isolated domains in which the stoichiometry between RCs and mobile carriers as PQ or PC is variable. As an example, diffusion of PQ within the appressed region is restricted to small domains of variable size, including an average of three to four RCs, but with widely different PSII/PQ ratio (21, 22). More recently, Kirchhoff *et al.* (25) measured in thylacoids and leaves low apparent equilibrium constants between P_{700}, PC, and cyt f. This disequilibrium, only found *in vivo* or in stacked thylacoids was interpreted by a restricted long-range PC diffusion.

In this paper, we have developed a method to quantify the relative fraction of PSI involved in cyclic and linear processes. Our previous measurements performed under saturating light (8) gave no access to this parameter, because the rate of the cyclic process is limited by dark processes (likely cyt bf turnover) and not by the rate of PSI. Thus, experiments were performed under conditions where the rate of the photosynthetic process is light-limited. When the electron transfer chain operates in the linear mode, the electrons formed on PSI acceptor side are transferred to NADP, and then to the Benson–Calvin cycle. As with far-red illumination, the rate of electron flow from PSII to PSI is negligible, P_{700} oxidation should occur after a lag phase associated with the oxidation of PSI secondary donors. On the contrary, in the cyclic mode, electrons are transferred back to P_{700}, through Fd and the cyt bf complex. In this case, P_{700} oxidation could only be associated with slow electron leaks from the cyclic chain (8).

Analysis of the kinetics of P_{700} and PC oxidation led us to propose a model in which thylacoids include three types of

Abbreviations: cyt, cytochrome; cyt bf, cytochrome b_6/f; Fd, ferredoxin; FNR, Fd-NADP oxidoreductase; MV, methylviologen; PC, plastocyanin; PQ, plastoquinone; PS, photosystem.

*To whom correspondence should be addressed. E-mail: pjoliot@ibpc.fr.

© 2005 by The National Academy of Sciences of the USA

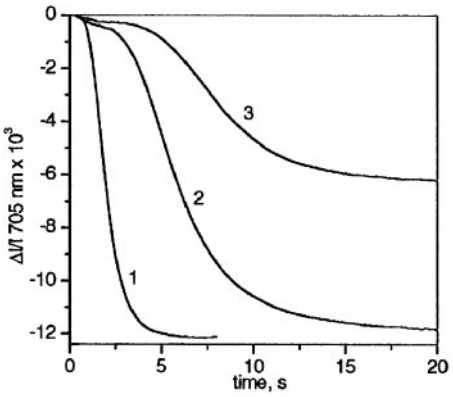

Fig. 1. Kinetics of P_{700} oxidation measured at 705 nm in dark-adapted infiltrated leaves. $K_{i\ PSI} \approx 6.5 \times 10\ s^{-1}$. Curve 1, 150 mM sorbitol plus 1 mM MV. Curve 2, 150 mM sorbitol plus 40 μM 3-(3,4-dichloro-phenyl)-1,1-dimethylurea plus 2 mM hydroxylamine. Curve 3, 150-mM sorbitol.

compartments out of equilibrium. This model, based on the organization of the photosynthetic chain proposed by Albertsson (26, 27), takes into account the low apparent equilibrium constant measured between the carriers of the photosynthetic chain.

Materials and Methods

Experiments were performed with pea leaves (*Pisum sativum*) grown in the laboratory and market spinach leaves (*Spinacea oleacera*). When required, 3-(3,4-dichloro-phenyl)-1,1-dimethylurea and hydroxylamine or methylviologen (MV) have been introduced by infiltration of the leaf by depression in the presence of 150 mM sorbitol to avoid osmotic shock (Fig. 1).

A technique for absorption and fluorescence measurements has been developed in collaboration with D. Béal (see *Supporting Text*, which is published as supporting information on the PNAS web site). In this apparatus, the absorption is sampled by detecting flashes provided by light-emitting diode (LEDs) that deliver 10-μs square pulses. This duration defines the time resolution of the method. Actinic far-red excitation is provided by LED peaking at 720 nm filtered through three Wratten filters 55 that block wavelengths shorter than 700 nm. Green actinic excitation is provided by LEDs peaking at 530 nm.

To protect the photodiode from the actinic light, far-red illumination is switched off during periods of 150 μs during which detecting flashes at 705 or 870 nm are fired. A fluorescence signal (less than $\approx$4% of P_{700} signal) is subtracted from absorption changes at 705 nm.

The absorption changes associated with P_{700} redox changes are computed as $\Delta I/I\ P_{700} = \Delta I/I\ 705\ nm - \Delta I/I\ 870\ nm/2$. $\Delta I/I$ PC is computed as $\Delta I/I\ 870\ nm + \Delta I/I\ 705\ nm/10$. These computations take into account the larger optical path at 870 nm as compared with 705 nm (see *Supporting Text*). Absorption changes at 705 nm display very similar kinetics to those associated with P_{700} redox changes, thus showing that measurement at 705 nm essentially reflects P_{700} oxidation (Fig. 2*A* and *B*). Owing to the low noise level of this technique ($\Delta I/I \approx 6 \times 10^{-6}$), the averaging of several experiments was not required.

Results

Infiltrated Leaves. Fig. 1 shows data obtained with three pieces from the same spinach leaf that display similar P_{700} oxidation kinetics before infiltration. In curve 1, a dark-adapted piece infiltrated with 150 mM sorbitol plus 1 mM MV was submitted to 30 s of far-red illumination ($K_{i\ PSI} \approx 6.5\ s^{-1}$), leading to P_{700} oxidation in $\approx$4 s. Because MV is able to accept electrons from all PSI, the photosynthetic chain operates according to the linear mode only. Thus, kinetics of P_{700} oxidation is limited by PSI primary and secondary donors' oxidation. In curve 2, another piece was infiltrated with 150 mM sorbitol plus 40 μM 3-(3,4-dichloro-phenyl)-1,1-dimethylurea plus 2 mM hydroxylamine. Kinetics of P_{700} oxidation were slower (completed in $\approx$20 s), although the final level of P_{700}^+ was approximately equal in curves 1 and 2. We ascribe the slow oxidation in the absence of MV to an efficient reinjection of electrons to P_{700} via the cyclic pathway. Electron leaks from the cyclic chain associated with electron transfer to oxygen (Mehler reaction) or with the Benson–Calvin cycle lead to a progressive P_{700} oxidation, as proposed in refs. 7 and 8. In curve 3, a third piece was infiltrated with 150 mM sorbitol. The level of P_{700}^+ reached after $\approx$20 s illumination is approximately two times smaller than in curves 1 and 2, showing that cyclic flow operates at approximately half of its initial rate. This finding implies that the slow electron flow generated by PSII under far-red excitation partially compensates the electron leaks from the cyclic chain. When the leaf is illuminated in green light that excites both PSI and PSII, electrons arising from PSII maintain P_{700} reduced, and the cyclic process operates for >20 s close to its maximum rate (data not shown).

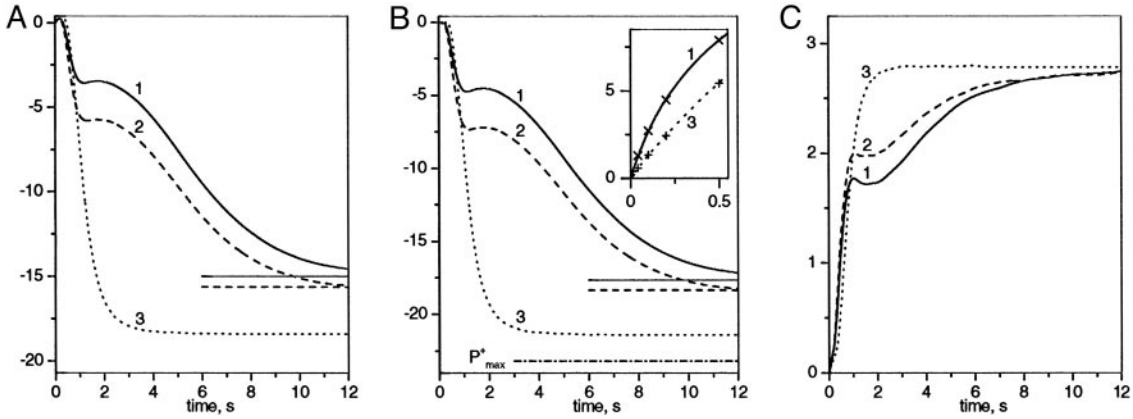

Fig. 2. Kinetics of P_{700} and PC oxidation measured in pea leaf submitted to far-red illumination. $K_{i\ PSI} \approx 8.4 \times 10\ s^{-1}$. (*A*) Absorption changes were measured at 705 nm. (*B*) Kinetics of P_{700} oxidation. (*B Inset*) Kinetics of P_{700}^+ reduction after 20 s of far-red illumination in conditions of curves 1 and 3 in *B*. (*C*) Kinetics of PC oxidation. Ordinate is expressed in $\Delta I/I \times 10^3$. Measurements at 870 and 520 nm (fluorescence) are not shown. Curves 1 and 2. To reach reproducible kinetics, the dark-adapted leaf was submitted to cycles of 20 s of far-red light, 5 min of dark, 20 s of far-red light, and 20 min of dark. Curves 1 and 2 are obtained after 20 and 5 min of dark, respectively. Curve 3, cycles of 10 min of green light, 5 min of dark, and 20 s of far-red light. Dash-dotted line, P^+_{max} (see text).

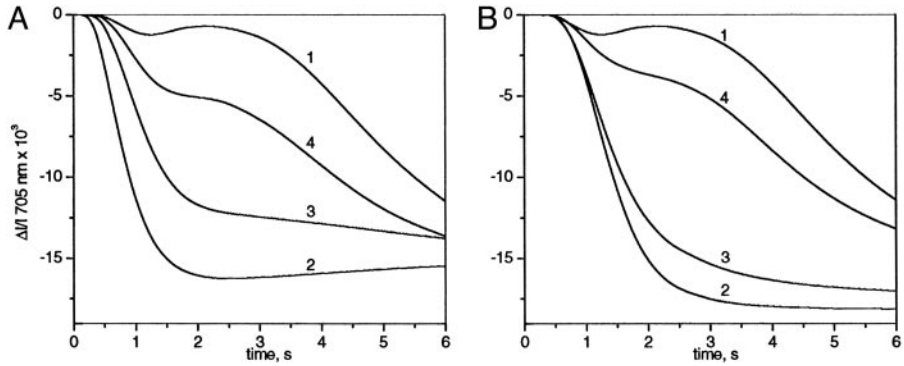

Fig. 3. Kinetics of P_{700} oxidation measured at 705 nm as a function of the time of dark-adaptation after illumination. $K_{i\ PSI} \approx 8.4 \times 10\ s^{-1}$. (*A*) The leaf was submitted to dark and light periods as follows: dark-adaptation (≈3 h), 20 s of far-red light (curve 1), 1 min of dark, and 20 s of far-red light (curve 2), 20 min of dark, 20 s of far-red light, 3 min of dark, and 20 s of far-red light (curve 3), 20 min of dark, 20 s of far-red light, 6 min of dark, and 20 s of far-red light (curve 4). (*B*) Curve 1, dark-adapted leaf. Curves 2, 3, and 4, >10-min strong green light plus 15, 25, and 43 min of dark, respectively.

Cyclic and Linear Flows in Dark-Adapted or Preilluminated Noninfiltrated Leaves. In Fig. 2, a pea leaf was submitted to 20 s of far-red illumination ($K_{i\ PSI} \approx 8.4\ s^{-1}$), and the absorption changes were measured at 705 (Fig. 2*A*) and at 870 nm (data not shown). It is worth pointing out that similar kinetics of P_{700} oxidation are observed when the same leaf is attached to or cut from the plant. Kinetics of the photo-induced redox changes of P_{700} and PC (Fig. 2 *B* and *C*, respectively) were computed as described in *Materials and Methods* and *Supporting Text*. Fig. 2, curve 1 (dark-adapted leaf) displays two phases, completed in ≈2 and ≈20 s, respectively. The amplitude of the two phases is roughly unchanged when the light intensity is decreased or increased by a factor of two (not shown). Thus, the biphasic P_{700} oxidation is not linked to a competition between light and dark processes, but rather, to the presence of two isolated membrane domains. We propose that the domains in which P_{700} is rapidly oxidized contain an excess of PSI_{linear}, whereas those in which P_{700} is slowly oxidized have an excess of PSI_{cyclic}. After 5 min of dark, following 20 s of far-red illumination (curves 2), the kinetics of P_{700} oxidation remains biphasic, but the relative amplitude of the fast phase is larger than that observed with the dark-adapted leaf, which suggests a larger concentration of PSI_{linear}.

In Fig. 2, curve 3, the leaf was preilluminated with green light (close to saturating excitation) for >10 min, a time long enough to fully activate the Benson–Calvin cycle. One thus expects the photosynthetic chain to operate mainly in the linear mode. After 5 min of dark, the leaf was submitted to far-red illumination that led to a monophasic oxidation of P_{700}, completed in ≈3 s. The kinetics are similar to that observed in the presence of MV, showing that most of PSI is still involved in the linear process. The maximum amount of P_{700}^+ (P^+_{max}) is computed, assuming that, when P_{700}^+ has reached its steady-state value (P^+_S), the rates of P_{700} oxidation and P_{700}^+ reduction are equal. The rate of P_{700} oxidation is proportional to the concentration of P_{700} that is equal to $P^+_{max} - P^+_S$. At the time the light is switched off, the rate of P_{700}^+ reduction is proportional to the initial slope of curve 3 (Fig. 2*B Inset*). We have

$$R = \approx 15.6 \times 10^{-3}\ s^{-1} = (P^+_{max} - P^+_S) \times K_{i\ PSI}$$

$$P^+_{max} = R/K_{i\ PSI} + P^+_S$$

$$= \approx 15.6 \times 10^{-3}\ s^{-1} / \approx 8.4\ s^{-1} + \approx 21.4 \times 10^{-3}$$

$$= \approx 23.3 \times 10^{-3}.$$

PSI turnover beyond ≈6 s of far-red illumination is ≈8% of that measured under condition that P_{700} is fully reduced. This value is consistent with the expected rate for the linear flow, because under far-red illumination, PSII antenna captures <10% of the absorbed photons. In the case of a dark-adapted leaf (Fig. 2*B*, curve 1), PSI turnover after 20 s of far-red illumination is approximately three times larger than for preilluminated leaf, and is mainly associated with the cyclic process. A similar estimate of PSI turnover is obtained when measuring rate of P_{700}^+ reduction, which is approximately three times larger in dark-adapted than in preilluminated leaf (Fig. 2*B Inset*, curves 1 and 3).

Kinetics of PC redox change in dark-adapted leaf (Fig. 2*C*, curve 1) displayed two phases with larger relative amplitude of the fast phase as compared with P_{700} oxidation.

Transition Between Linear and Cyclic Modes. Fig. 3*A* displays the kinetics of P_{700} oxidation measured at 705 nm with a pea leaf dark-adapted for ≈3 h (curve 1) or after 1, 3, or 6 min of dark after 20 s of far-red illumination (curves 2, 3, and 4, respectively). It is worth noting that in this particular leaf, the amplitude of the fast phase is smaller than in the experiments shown in Fig. 2. The duration of the lag phase increases with the dark period to reach its maximum value after ≈6 min of dark. Because the duration of the lag phase is an increasing function of the concentration of low potential PSI secondary donors (PQH_2 plus cyt f plus Rieske protein), we conclude that electron transfer from the stroma to the secondary PSI acceptors is a slow process completed in ≈6 min. Curve 2 (1 min of dark) displayed a fast P_{700} oxidation kinetics, showing that a 20-s far-red illumination converts a fraction of PSI_{cyclic} in PSI_{linear}. Then, the amplitude of the fast phase decreases with the time of dark-adaptation to reach after ≈20 min of dark (data not shown), a value similar to that measured after ≈3 h of dark (curve 1). The half-time for the conversion in the dark of PSI_{linear} into PSI_{cyclic} is ≈4 min. In Fig. 3*B*, the same leaf as that used in Fig. 3*A* was illuminated under strong green light for >10 min to induce the transition PSI_{cyclic} to PSI_{linear}, followed by 15, 25, and 43 min of dark (curves 2, 3, and 4, respectively). The half-time for the reverse conversion (≈30 min) is approximately seven times longer than that measured after 20 s of far-red illumination. It is worth pointing out that faster transitions are observed for preillumination periods <10 min.

Variability Among Leaves. Kinetics of P_{700} oxidation are extremely variable among dark-adapted leaves. Fig. 4*A* shows the kinetics of P_{700} oxidation measured in different pea leaves from plants grown simultaneously under the same conditions. Curves 1–3 displayed fast and slow phases with variable relative amplitude and kinetics, which implies different values of $PSI_{cyclic}/PSI_{linear}$ ratio. In other pea leaves, monophasic P_{700} oxidation kinetics

PLANT BIOLOGY

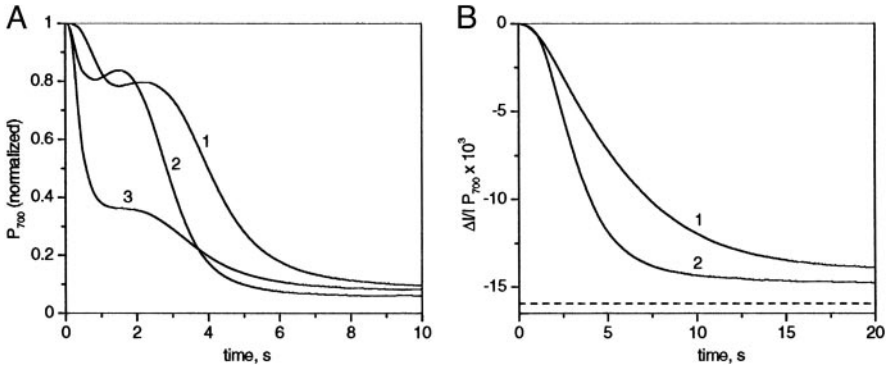

Fig. 4. Kinetics of P_{700} oxidation measured at 705 nm with different leaves. (*A*) Dark-adapted pea leaf. The kinetics is normalized to the total amount of P_{700}. ($K_{i\ PSI} \approx 8.4 \times 10\ s^{-1}$). (*B*) Spinach leaf ($K_{i\ PSI} \approx 3.9 \times 10\ s^{-1}$). Curve 1, dark-adapted leaf. Curve 2, leaf illuminated for >10 min in strong green light plus 10 min of dark. The redox change of P_{700} is computed from 705, 870, and 520 nm (fluorescence) measurements (data not shown). Dashed line, P^{+}_{max}.

with various half-times were observed (data not shown). It is worth pointing out that monophasic or biphasic kinetics were also observed for different C3-plants as *Arabidopsis*, periwinkle, spinach, or a tree (false acacia). A monophasic kinetics of P_{700} oxidation with a dark-adapted spinach leaf is shown Fig. 4*B*, curve 1. A faster P_{700} oxidation was observed when the same leaf was preilluminated for 10 min in strong green light followed by 15 min of dark (Fig. 4*B*, curve 2). This finding shows that in this dark-adapted leaf, a significant fraction of PSI is also involved in the cyclic process.

Discussion

Compartmentation. Fig. 5 shows the function $[PC^+] = f[P_{700}^+]$ computed from data of Figs. 2 *B* and *C* and 4*B*. This function is identical for preilluminated spinach or pea leaf (curve 1). The same function is obtained when spinach leaf is illuminated at higher intensity ($K_{i\ PSI} \approx 8.4\ s^{-1}$, data not shown). Curve 1 largely differs from the theoretical function (curve 4) computed from the redox potential midpoints of P_{700} and PC. The apparent equilibrium constant computed from curve 1 (≈4) is approximately seven times lower than the theoretical value (≈40). Low equilibrium constants were also measured with dark-adapted leaves (curves 2 and 3). We thus conclude that electron carriers involved in the photosynthetic electron transfer chain are included in different membrane compartments not in thermodynamic equilibrium. The independence of the apparent equilibrium constant with respect to light intensity implies that the carriers included in a given compartment are in thermodynamic equilibrium, and that there is no PC diffusion between compartments in a time range of several tens of seconds. This conclusion differs from that of Kirchhoff *et al.* (25) who proposed a limitation by the rate of lateral diffusion of PC. This contradiction may arise from the difference in the time range of our experiments and that of Kirchhoff *et al.* (25), i.e., ≈20 s and a few hundreds of milliseconds, respectively. Irrespective of the PC/PSI ratio in the different compartments, PC oxidation at the onset of illumination should precede that of P_{700}, owing to the high value of the local equilibrium constant between these two carriers. This result explains why the initial slopes of curves 1–3 are close to that of curve 4. During the course of illumination, P_{700} oxidation in compartments with low PC/PSI ratio should occur before completion of PC oxidation in compartments with high PC/PSI ratio. The coexistence of P_{700}^+ with reduced PC leads to a low apparent equilibrium constant when averaging the concentration of the carriers in all compartments. This model predicts the nonhyperbolic character of curves 1–3. Another example of low apparent equilibrium constant in the photosynthetic chain was given ≈40 years ago (18) in experiments using thylacoids submitted to weak illumination in the presence of MV. The apparent equilibrium constant between primary PSII acceptor Q_A and P_{700} was close to ≈5, whereas the value computed from the midpoint potential of these two carriers is $>10^7$. As proposed by J. Lavergne (personal communication), these results could be interpreted assuming that chloroplasts include compartments with different PSI/PSII stoichiometry. Let us assume that chloroplasts include a first compartment with 0.3 PSI and 0.7 PSII and a second compartment with 0.7 PSI and 0.3 PSII. During subsaturating illumination that excites equally PSI and PSII, the concentration of the active form of reaction centers in each compartment adjust until an equal rate of PSI and PSII photoreactions is reached, i.e., $[P_{700}] = [Q_A]$. Because of the large equilibrium constant between P_{700} and Q_A (10^7), P_{700}^+ and Q_A^- cannot coexist in a same compartment and $[P_{700}] = [Q_A] = 0.3$ in each compartment. Thus, if one sums the concentration of each redox state of Q_A and P_{700} in the two compartments, we obtain $[Q_A] = [P_{700}] = 2 \times 0.3 = 0.6$ and $[Q_A^-] = [P_{700}^+] = 1 - 0.6 = 0.4$. The apparent equilibrium constant is then $K = [Q_A]/[Q_A^-] \times [P_{700}]/[P_{700}^+] = 0.6/0.4 \times 0.6/0.4 = 2.25$, a value that is by far $<10^7$.

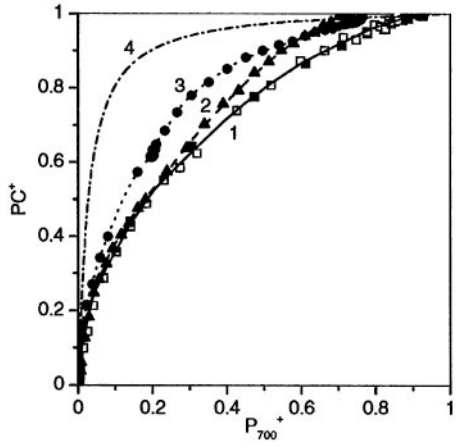

Fig. 5. $PC^+ = f(P_{700}^+)$ during far-red illumination. Curve 1, □, computed from Fig. 2 *B* and *C*, curves 3; ■, computed from Fig. 4*B*, curve 2. Curve 2, computed from Fig. 4*B*, curve 1. Curve 3, computed from Fig. 2 *B* and *C*, curves 1. Curve 4, theoretical function assuming a midpoint redox potential of 465 and 330 mV for P_{700} and PC, respectively.

What could be the structural support for such variability in the PSI/PSII functional stoichiometry? Stroma lamellae form helicoidal ramps that connect successive levels of a grana stack by means of a series of narrow junctions (frets) (28, 29). If PC is unable to diffuse through the fret junctions, the vesicles super-

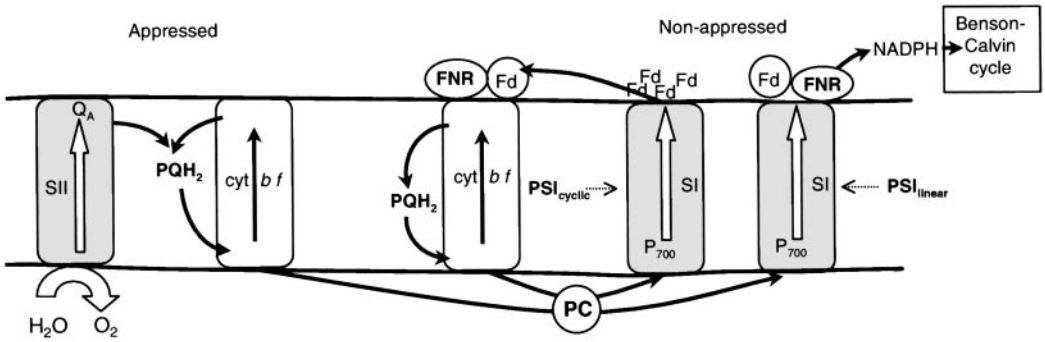

Scheme 1. Lateral organization of the thylacoid membrane.

imposed in the grana stacks are isolated one from the other, thus forming compartments out of thermodynamic equilibrium. Our interpretation, as in ref. 25, is based on the organization of the photosynthetic membrane proposed in (26, 27). In this model, PSI is included in three nonappressed membrane regions, the margin and end membranes of the grana stacks, and the stroma lamellae. We can then distinguish three types of compartments with different PSI/PSII stoichiometry. Compartment A is formed by vesicles localized inside the grana stacks. Each vesicle includes two appressed surfaces and the margin that represents only ≈40% of the total membrane surface. Thus, compartment A includes more PSII than PSI. Compartment B localized at the top and bottom of the grana stacks includes a large nonappressed surface (margin and end membranes) and a single appressed surface, leading to a PSI/PSII ratio higher than in compartment A. The third compartment is formed by the stroma lamellae that includes two membrane domains with a PSI/PSII ratio of ≈3.1 and ≈13, respectively (30). This model provides a structural basis for the variable PSI/PSII stoichiometry proposed by J. Lavergne (personal communication). If one assumes that PC is equally distributed along all of the membrane surfaces, the PSI/PC ratio in each compartment will be approximately proportional to the ratio between the nonappressed and the total membrane surface. This ratio is much larger in compartment B and stroma lamellae than in compartment A, thus providing a structural basis for different PSI/PC stoichiometries.

Distribution of PSI_{linear} and PSI_{cyclic} Within the Membrane. In the case of the biphasic kinetics shown in Fig. 2 *B* and *C*, curves 1, ≈20% of P_{700} and ≈60% of PC are oxidized during the fast phase, whereas ≈80% of P_{700} and ≈40% of PC are oxidized during the slow phase. This finding points to two independent domains with the paradox that P_{700} oxidation is faster in the domains that include a large amount of PSI secondary donors (large PC/PSI ratio) than in the domains with a small amount of donors (low PC/PSI ratio). As proposed above, it implies that the linear and cyclic processes occur preferentially in the fast and slow domains, respectively. Thus, in the case of biphasic kinetics that are the most commonly observed, it is possible on the basis of PC/PSI stoichiometry to draw correlation between these domains and the compartments as defined in the preceding paragraph. The fast domains correspond to the grana stacks (compartment A), whereas the slow domains correspond to the stroma lamellae and compartment B. It is worth pointing out that the size of the antenna associated with PSI is ≈1.4 times larger in grana margins than in stroma lamellae (30). This finding implies that $K_{i\ PSI}$ is ≈1.4 times larger in the grana stacks than in the stroma lamellae. This localization of linear and cyclic chains within the chloroplast is similar to those previously proposed (8, 25, 27).

A different distribution of PSI_{linear} and PSI_{cyclic} among the compartments must be assumed in the case of a leaf that displays monophasic kinetics of P_{700} oxidation (Fig. 4*B*). In this case, we propose that a dark-adapted leaf includes PSI_{linear} and PSI_{cyclic} approximately evenly distributed in the different compartments. In other terms, cyclic and linear flows will occur both in the stroma lamellae and in the grana stack compartments. In Scheme 1, all compartments include PSI_{linear} and PSI_{cyclic}, at variance with the model we previously proposed (scheme 2 in ref. 8). According to Scheme 1, the rate of P_{700} oxidation depends on the number of reduced PSI secondary donors and on the probability for reduced PC to bind PSI_{linear}. If one assumes that PC establishes a thermodynamic equilibrium between P_{700} belonging to PSI_{linear} and PSI_{cyclic}, this probability is proportional to the PSI_{linear}/PSI_{total} ratio. In Fig. 4*B*, the duration of the lag phase that reflects the concentration of secondary donors is similar in dark-adapted (curve 1) and preilluminated leaf (curve 2). Thus, the PSI_{linear}/PSI_{total} ratio can be roughly estimated by comparing the half-time of curve 1(≈3.1 s) and curve 2 (≈5 s). Assuming that the preilluminated leaf includes PSI_{linear} only, we estimate that the dark-adapted leaf includes ≈3.1/≈5 = ≈0.62 PSI_{linear} and ≈0.38 PSI_{cyclic}. The P_{700} oxidation kinetics shown in Fig. 1, curves 2 and 3, and Fig. 3, curve 1, are slower than that in Fig. 4*B*, curve 1. Following the same line of interpretation, comparison of the half-time of curves 1 and 2, Fig. 1, leads us to estimate that the dark-adapted leaf includes ≈0.3 PSI_{linear} and ≈0.7 PSI_{cyclic}. An alternate hypothesis is that at least a part of the slow P_{700} oxidation is associated with the oxidation of Fd through a soluble FNR or by oxygen (Mehler reaction). In this last case, the radical species generated will be eliminated by peroxidases present in the chloroplast. If all of the slow P_{700} oxidation is associated with Fd oxidation, the concentration of PSI_{cyclic} in Figs. 1, curves 2–3, and 3*A*, curve 1, is close to 100%.

Regulation. We showed that in dark-adapted leaves, a fraction of PSI is involved in the cyclic process, whereas, as proposed by Sacksteder and Kramer (31) and Harbinson *et al.* (32), preilluminated leaves operate according to the linear mode. What can be the physiological parameters that control this conversion that we associate with the release of FNR from PSI? It could be controlled by the redox poise of the stromal compartment through a process similar to the control of the thioredoxin-dependent enzymes. Owing to the large efficiency of the cyclic process, far-red illumination generates very few electrons in the stromal compartment. Because such an illumination is able to induce PSI_{cyclic} to PSI_{linear} conversion, this hypothesis appears unlikely. As in ref. 7, we favor that this conversion is induced by the increase in ATP concentration associated with the cyclic process. The 10-min strong illumination gives enough time for equilibration between the cell and the chloroplasts of the large light-induced increase of ATP concentration. The accumulation of a large ATP pool would explain the long lifetime of PSI_{linear}. Interestingly, the conversion of linear into cyclic mode in the

dark starts after a lag period of ≈20 min, whereas it is likely that the concentration of ATP has already decreased during this time interval. This finding suggests that the transition occur in a narrow range of ATP concentration (threshold level), and it could explain why a far-red excitation that generates a smaller increase of the ATP pool induces a large PSI_{cyclic} to PSI_{linear} conversion but with a faster reverse conversion in the dark.

We are not able to explain the large variations in the amount and distribution of PSI_{cyclic} and PSI_{linear} in dark-adapted leaves. Assuming that the concentration of ATP in the dark is close to the threshold level, rather small changes in the ATP concentration in dark-adapted leaves would be associated with large variations of the relative concentration of PSI_{cyclic} and PSI_{linear}.

A quantitative analysis of the effect of ATP concentration on the transition between the linear and cyclic mode is definitely required to test our working hypothesis.

We thank F. Rappaport and G. Finazzi for their critical reading of the manuscript and valuable suggestions. This work was supported by the Centre National de la Recherche Scientifique (Unité Mixte de Recherche 7141) and the Collège de France (Paris).

1. Arnon, D. I., Whatley, F. R. & Allen, M. B. (1955) *Biochim. Biophys. Acta* **16,** 607–608.
2. Tagawa, K., Tsujimoto, H. Y. & Arnon, D. I. (1963) *Proc. Natl. Acad. Sci. USA* **49,** 567–572.
3. Maxwell, P. C. & Biggins, J. (1976) *Biochemistry* **15,** 3975–3981.
4. Joët, T., Cournac, L., Peltier, G. & Havaux, M. (2002) *Plant Physiol.* **128,** 760–769.
5. Asada, K., Heber, U. & Schreiber, U. (1993) *Plant Cell Physiol.* **34,** 39–50.
6. Burrows, P. A., Sazanov, L. A., Svab, Z., Maliga, P. & Nixon, P. J. (1998) *EMBO J.* **17,** 868–876.
7. Joliot, P. & Joliot, A. (2002) *Proc. Natl. Acad. Sci. USA* **99,** 10209–10214.
8. Joliot, P., Beal, D. & Joliot, A. (2004) *Biochim. Biophys. Acta* **1656,** 166–176.
9. Sazanov, L. A., Burrows, P. & Nixon, P. J. (1995) in *Photosynthesis: From Light to Biosphere. Xth International Congress on Photosynthesis*, ed. Mathis, P. (Kluwer, Montpellier, France), Vol. 2, pp. 705–708.
10. Stroebel, D., Choquet, Y., Popot, J.-L. & Picot, D. (2003) *Nature* **426,** 413–418.
11. Kurisu, G., Zhang, H. M., Smith, J. L. & Cramer, W. A. (2003) *Science* **302,** 1009–1014.
12. Clark, R. D., Hawkesford, M. J., Coughlan, S. J., Bennett, J. & Hind, G. (1984) *FEBS Lett.* **174,** 137–142.
13. Zhang, H. M., Whitelegge, J. P. & Cramer, W. A. (2001) *J. Biol. Chem.* **276,** 38159–38165.
14. Andersen, B., Scheller, H. V. & Moller, B. L. (1992) *FEBS Lett.* **311,** 169–173.
15. van Thor, J. J., Geerlings, T. H., Matthijs, H. P. & Hellingwerf, K. J. (1999) *Biochemistry* **38,** 12735–12746.
16. Scheller, H., Jensen, P., Haldrup, A., Lunde, C. & Knoetzel, J. (2001) *Biochim. Biophys. Acta* **1507,** 41–60.
17. Naver, H., Scott, N., Andersen, B., Moller, B. & Scheller, H. (1995) *Physiol. Plant.* **95,** 19–26.
18. Joliot, P., Joliot, A. & Kok, B. (1968) *Biochim. Biophys. Acta* **153,** 635–652.
19. Kok, B., Joliot, P. & McGloin, M. (1969) in *Progress in Photosynthesis Research*, ed. Metzner, H. (International Union of Biological Sciences, Tubingen, Germany), Vol. 2, pp. 1042–1056.
20. Joliot, P. & Joliot, A. (1984) *Biochim. Biophys. Acta* **765,** 210–218.
21. Joliot, P., Lavergne, J. & Béal, D. (1992) *Biochim. Biophys. Acta* **1101,** 1–12.
22. Lavergne, J., Bouchaud, J. P. & Joliot, P. (1992) *Biochim. Biophys. Acta* **1101,** 13–22.
23. Kirchhoff, H., Horstmann, S. & Weis, E. (2000) *Biochim. Biophys. Acta* **1459,** 148–168.
24. Lavergne, J. & Joliot, P. (1991) *Trends Biochem. Sci.* **16,** 19–134.
25. Kirchhoff, H., Schottler, M. A., Maurer, J. & Weis, E. (2004) *Biochim. Biophys. Acta* **1659,** 63–71.
26. Albertsson, P. A. (1995) *Photosynth. Res.* **46,** 141–149.
27. Albertsson, P. A. (2001) *Trends Plant Sci.* **6,** 349–354.
28. Brangeon, J. & Mustardy, L. (1979) *Biol. Cell.* **36,** 71–80.
29. Mustardy, L. & Garab, G. (2003) *Trends Plant Sci.* **8,** 117–122.
30. Danielsson, R., Albertsson, P. A., Mamedov, F. & Styring, S. (2004) *Biochim. Biophys. Acta* **1608,** 53–61.
31. Sacksteder, A. & Kramer, D. M. (2000) *Photosynth. Res.* **66,** 145–158.
32. Harbinson, J., Genty, B. & Baker, N. R. (1990) *Photosynth. Res.* **25,** 213–224.